Results in Physics 7 (2017) 3552–3556

Contents lists available at ScienceDirect

Results in Physics

journal homepage: www.journals.elsevier.com/results-in-physics

Synthesis and length dependent photoluminescence property of zinc oxide nanorods

Ishaq Musa [a,*], Naser Qamhieh [b], Saleh Thaker Mahmoud [b]

[a] Department of Physics, Palestine Technical University-Kadoorie, Tulkarm, P.O. Box 7, Palestine
[b] Department of Physics, UAE University, Al-Ain, P.O. Box 15551, United Arab Emirates

ARTICLE INFO

Article history:
Received 28 June 2017
Received in revised form 15 September 2017
Accepted 15 September 2017
Available online 21 September 2017

Keywords:
ZnO nanorods
Raman spectroscopy
UV–Vis spectroscopy
Photoluminescence spectroscopy

ABSTRACT

One-dimensional nanostructure ZnO nanorods (NRs) with controlled lengths and diameters were synthesized by the growth of colloidal nanoparticles and then characterized by XRD, TEM, Raman, PL and UV–Vis. The growth time parameter plays an important role in the formation process of ZnO NRs. The as-prepared nanoparticles has spherical shape with size about 4 nm, and formed single-crystalline NRs of length up to 150 nm and 16–20 nm in diameters. Raman spectra of the as-grown ZnO nanorods revealed the existence of Raman silent modes $B_1^{(low)}$ and $B_1^{(high)}$ at 273 and 538 cm^{-1} respectively. Photoluminescence (PL) and UV–visible absorption measurements have been performed at room temperature. The PL spectrum showed that the relative intensity of ultraviolet (UV) and defect bands depend on the length of ZnO nanorods. The peak of photoluminescence of UV band around 395 nm is strongly enhanced when the length of ZnO nanorods is reduced and the humps around 580 nm decreases.

Introduction

Zinc oxide (ZnO) is n-type semiconductor material of a wide band-gap (3.37 eV) at room temperature and has high exciton binding energy (60 meV) [1,2]. ZnO is a well-known luminescent material which can be applied in optoelectronic devices such as light emitting diodes, lasers, sensors [3–5], photovoltaic devices [6], and other promising applications in electroluminescent devices consisting of inorganic/organic materials [7], and recently in phase change memory devices [8]. In addition, ZnO exhibits two emission bands in the UV and visible regions at room temperature [9]. The first UV emission is located at 375 nm and a broader emission of the green spectral range occurs between 480 and 560 nm which reflects various types of intrinsic defects always are presented in the ZnO nanostructure [10]. The relative intensity of these bands depends on the type of fabrication process of ZnO such as; thin film [11], nanoparticles [12], nanorods [13,14], nanowires [15] and nano-flower [16]. In the last decade, various methods were employed to produce ZnO nanostructures with different sizes, shapes, and lengths, for example: sol-gel methods [17], pulsed laser deposition (PLD) [18], physical vapor deposition [19], and hydrothermal route [20,21]. Sol-gel method has been widely used to fabricate one-dimensional nanostructures [22]; it is a very attractive method due to its simplicity, large area, and low cost [19].

Cludia and co-workers [23] reported single crystalline ZnO nanorods structured from spherical ZnO nanoparticles. They observed ZnO nanorods with average length of 100 nm and width of approximately 15 nm.

Structural defects and growth variation of ZnO NRs are sensitive to Raman spectroscopy [24]. The Raman non active branches or silent modes such as $B_1^{(high)}$ and $B_1^{(high)}$ may become activated by introducing defects, or by doping with other elements [25]. The active and silent Raman modes have been studied theoretically [26,27], and experimentally. Serrano et al. [25], have observed the active and silent Raman modes by using inelastic neutron scattering (INS) experiment on a single crystals of ZnO.

In this work, we report the synthesis of various lengths of ZnO nanorods growth from colloidal nanoparticles. The length and diameter are based on the growth time of the formation process. The produced nanorods with different lengths are characterized by TEM, XRD, UV–visible absorption and photoluminescence spectrum. Moreover, Raman spectroscopy of active and inactive branches of optical phonon was studied and showed new features in the spectrum.

* Corresponding author.
E-mail address: i.musa@ptuk.edu.ps (I. Musa).

https://doi.org/10.1016/j.rinp.2017.09.035
2211-3797/

Experimental

ZnO nanorods at different growth times and with average lengths of 50–150 nm were synthesized by conducting the following steps. First, colloidal solution of ZnO was prepared to produce nanoparticles with an average diameter of 4 nm using Spanhel and Anderson method [17]. Briefly, a 5.5 g of zinc acetate dehydrate (98 +%, sigma Aldrich) in 250 ml of ethanol was heated until the solution became clear. This solution was refluxed for 1hr, and 150 ml of the solvent was removed by distillation and replaced by the same amount of fresh ethanol. Then, 1.39 g of lithium hydroxide monohydrate (Aldrich) was added to the solution in an ultrasonic bath at 0 °C. The mixture was dispersed for 1 h to obtain a transparent solution consisting of ZnO nanoparticles in suspension with apparent diameters of about 4 nm. The solution was filtered through a 0.1 μm membrane filter to remove undissolved LiOH. In the second step, Hoyer's method [28] was used with modifications. The solution of 100 ml containing ZnO nanoparticles was heated and mixed with 10% of deionized water at 60 °C for different periods of time 2, 6, 18, and 48 h. During this process, a white powder was formed and precipitated. Then the solution was centrifuged and washed four times with ethanol–water mixture (19:1) to remove physisorbed ionic compounds.

The shape and length of ZnO nanorods were analyzed using transmission electron microscope (TEM) using Tecnai G2 F20 Spirit BioTwin, Netherlands. Powder X-ray diffraction (XRD) patterns were obtained at room temperature using Shimadzu 6100 XRD and CuKα radiation (λ = 0.15406 nm). The optical absorption spectra were obtained using Jasco UV–Visible spectrophotometer. In order to get the phonon vibrational study of the ZnO nanorods XploRA confocal Raman microscope (Horiba Jobin Yvon, France) was used with laser excitation of 532 nm wavelength. Photoluminescence experiments were carried out by Varian Cary Eclipse Fluorescence Spectrophotometer with excitation wavelength 320 nm.

Results and discussion

TEM and XRD characterization

Morphology and particle size of the synthesized ZnO nanoparticles are shown in Fig. 1. The mean size estimated from the TEM image is about 4 nm. Fig. 2 shows the TEM images of ZnO nanorods with different growth time of 2, 6, 18, and 48 h. The TEM image shows that the average diameter of the nanorods varies from 16 nm for 2 h growth time to 20 nm for 48 h, and their lengths vary between 50 nm and 150 nm. The variation of the length and diameter of ZnO nanorods with the growth time was plotted in Fig. 3. The figure shows that the diameter and length are directly proportional with the growth time. Moreover, the selected area electron diffraction (SAED) in Fig. 2(e) obtained from TEM verified the crystal nature of the produced nanorods, and the bright uniform spots are confirming the preferential orientation for nanocrystals instead of random orientation.

More information about the crystal structure of the ZnO nanorods can be obtained from Fig. 4, which shows a typical XRD pattern of the as prepared ZnO nanorods at different growth time (2, 6, 18, and 48 h). The sharpness of the peaks implied the high crystallinity of the as-prepared ZnO nanorods with a single-phase nature of a wurtzite structure. The observed diffraction peaks can be attributed to the presence of pure hexagonal phase of ZnO with lattice constants of a = 3.251 Å and c = 5.208 Å. The data is in good agreement with JCPDS card for ZnO (JCPDS, 036-1451). It should be noted here that the full width at half maximum (FWHM) of the diffraction peaks increases when the growth time decreases. Consequently, the diameter of ZnO nanorods decreases. The full width

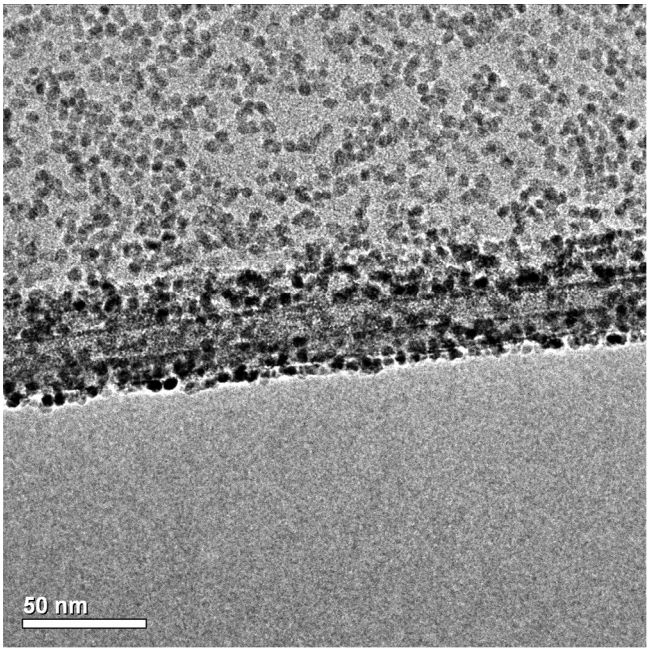

Fig. 1. TEM image of ZnO nanoparticles of size 4 nm.

at half maximum of the peak (0 0 2), in the XRD pattern is routinely used to determine the mean crystalline size using the De-bye-Scherer's formula [29],

$$D = \frac{0.9\lambda}{\beta \cos\theta} \tag{1}$$

where λ, θ, and β are the X-ray wavelength (0.154 nm), Bragg diffraction angle, and FWHM, respectively. The results of the crystalline diameter of ZnO nanorods are estimated to be 16, 16.2, 18.5 and 20 nm for growth times 2, 6, 18, and 48 h, respectively. These results are consistent with the results obtained from the TEM images in Fig. 2.

Raman spectroscopy

The optical phonons, Γ_{opt} in wurtzite crystals is given by $\Gamma_{opt} = 1A_1 + 2B_1 + 1E_1 + 2E_2$. Here A_1 and E_1 modes are polar and split into a transverse optical mode (TO) and a longitudinal optical mode (LO). E_2 mode consists of low $E_2^{(low)}$ and high $E_2^{(high)}$ frequency phonons modes. $E_2^{(low)}$ is associated with the vibration of oxygen atom and $E_2^{(high)}$ is related to heavy Zn sublattices [30]. In addition, the B_1 (low) and B_1 (high) modes are not Raman active. Fig. 5 shows Raman spectra of the ZnO nanorods. In this figure, the observed peaks at 98 and 437 cm^{-1} are assigned to $E_2^{(low)}$ and $E_2^{(high)}$ modes, respectively [31]; these are typical for the Raman active branches, which are attributed to the ZnO nonpolar optical phonons. The broad peaks appear at 273 and 538 cm^{-1} are assigned to silent $B_1^{(low)}$ [32] and $B_1^{(high)}$ modes respectively, which became activated by inducting defects [27,33]. The peak at 328 cm^{-1} corresponds to the second order Raman spectrum arising from zone boundary phonons (E_2 high – E_2 low) [24], while the peak at 584 cm^{-1} corresponds to the $1E_1$ (LO) mode of ZnO associated with oxygen deficiency [34]. The peak position at 208 cm^{-1} is assigned to the second-order $2E_2^{(low)}$ structure [33], and the peak at 385 cm^{-1} is attributed to A_1 (TO) mode [35]. Furthermore, phonon frequencies at 150 and 478 cm^{-1} are in excellent agreement with a reported theoretical calculations [25]. Additionally, Raman mode

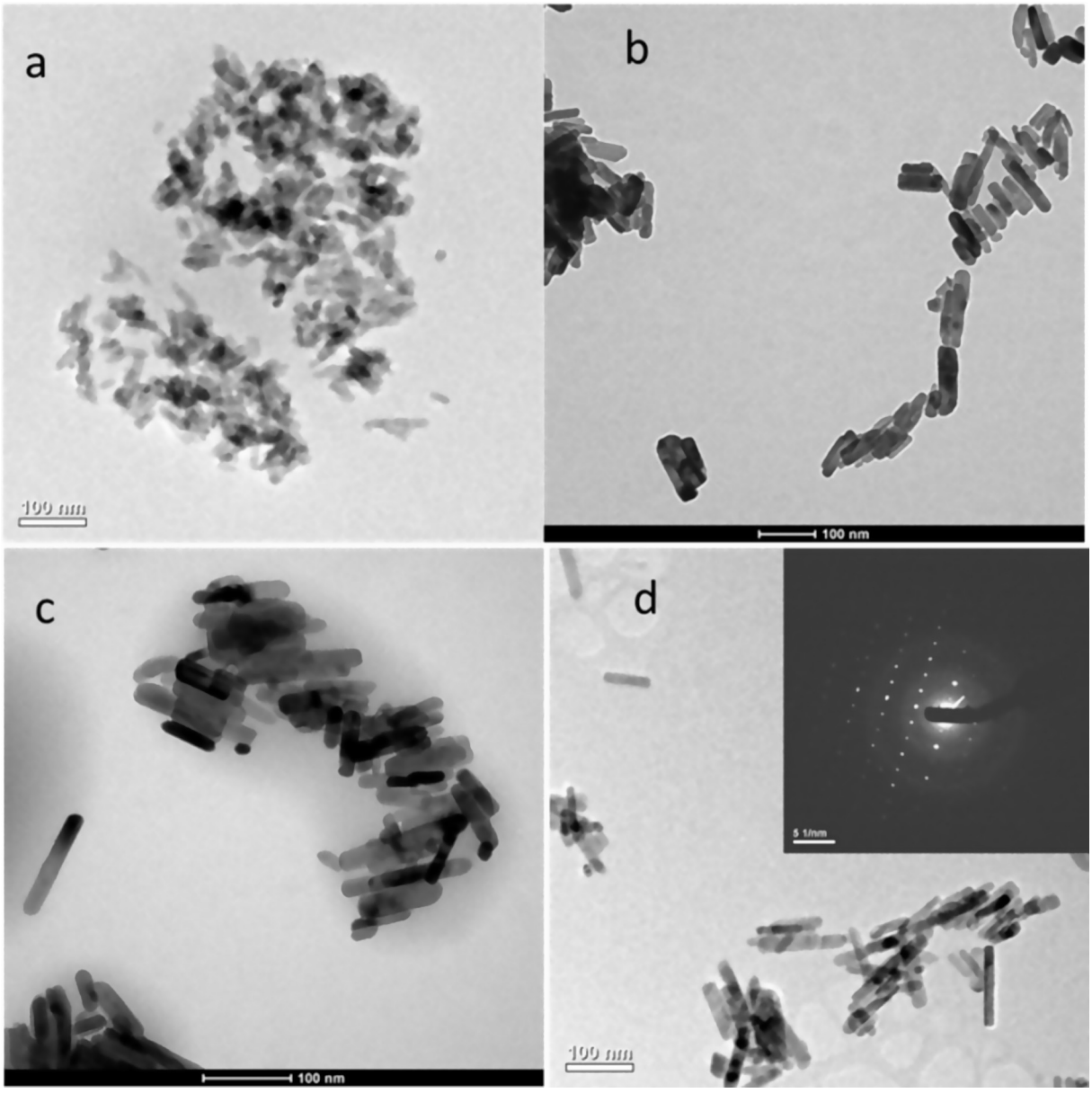

Fig. 2. TEM images of various length of ZnO nanorods growth in different times (a) 2 h (b) 6 h (c) 18 h (d) 48 h and the inset is for selected area electron diffraction (SAED) pattern of ZnO nanorods.

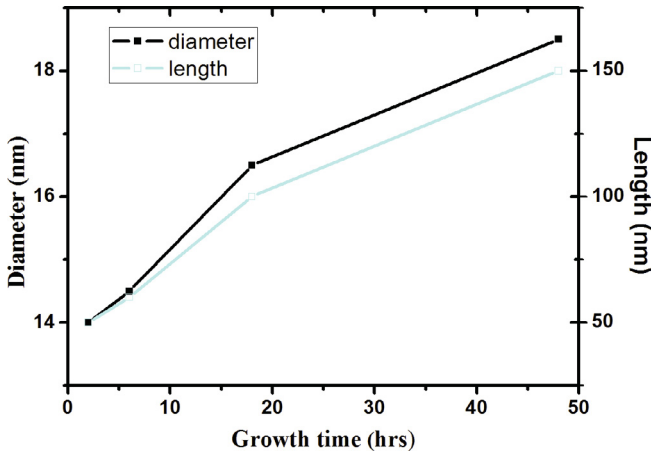

Fig. 3. Growth time of ZnO nanorods verses length and diameter.

observed at 683 cm^{-1} is originated from the acetate groups used as a reactants in the synthesis process, and ascribed to the O-C-O symmetric bends [36].

UV-absorption and photoluminescence

The room temperature UV–visible absorption spectra of ZnO nanorods for various growth times are shown in Fig. 6. It exhibits a strong absorption edge at about 367 nm (3.378 eV). The optical energy gap, E_g of the ZnO nanorods with different growth time can be determined by using the Tauc graphs [37], one can plot, $(\alpha h\nu)^2$ versus the photon energy $h\nu$ using the data obtained from the absorption spectra as shown in Fig. 7. It reveals that the obtained plotting gives tangent to the linear portion of the curves in a certain region. The energy gap (E_g) values is obtained by extending this straight line to intercept the ($h\nu$)-axis at $(\alpha h\nu)^2 = 0$. The band gap calculated for as-synthesized ZnO nanorods are (3.21, 3.18, 3.14, and 3.11 eV) for samples at 2, 6, 18 and

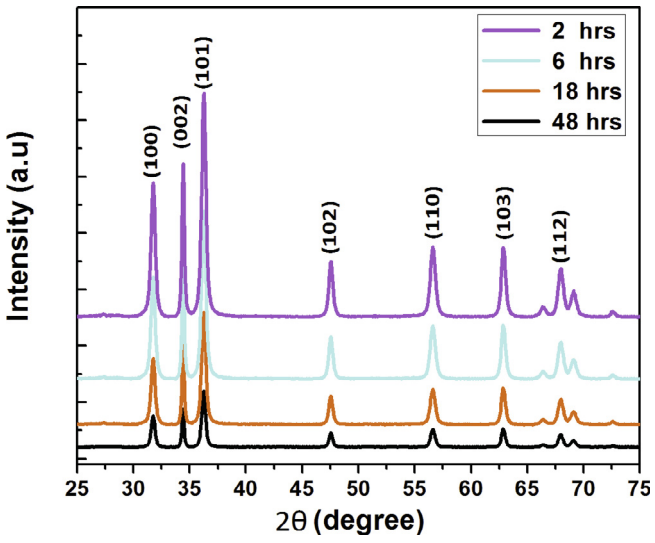

Fig. 4. XRD patterns of ZnO nanorods for various growth time (2, 6, 18, 48 h).

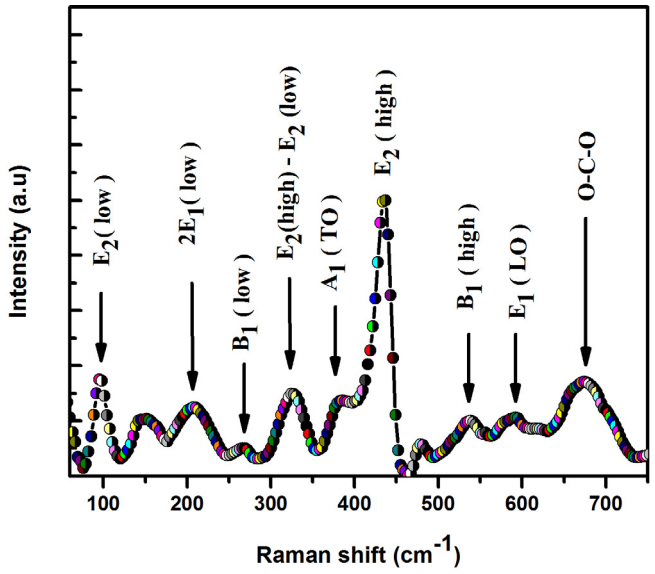

Fig. 5. Raman spectrum of the ZnO nanorods.

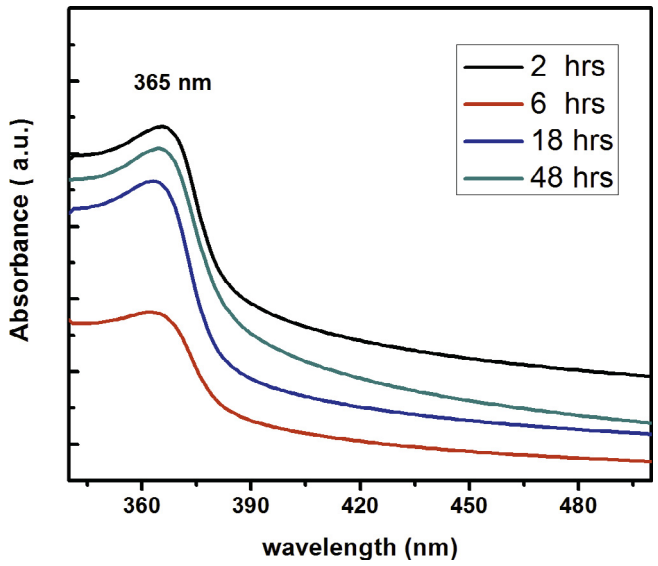

Fig. 6. Room temperature UV–Visible absorption spectra of ZnO nanorods for various growth times (2, 6, 18, 48).

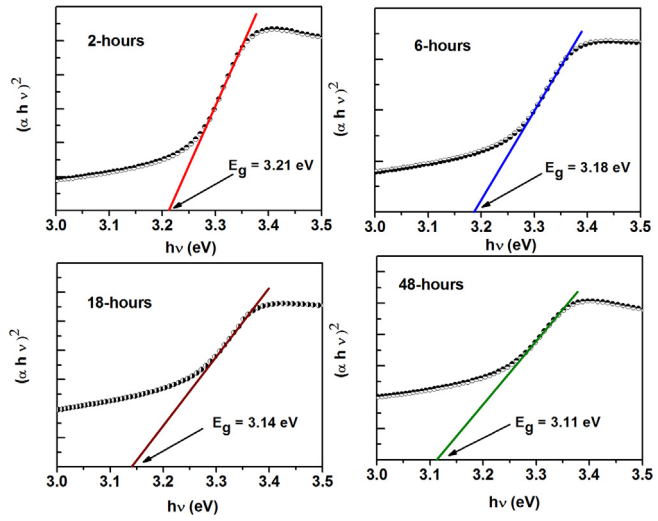

Fig. 7. Tauc plot: $(\alpha h\nu)^2$ as a function of photon energy for the ZnO nanorod prepared for different growth time (2, 6, 18, and 48 h).

48 h growth time, respectively. It is worth noting that the obtained Eg values are less than the band gap of bulk ZnO (3.37 eV). This results indicate that when the growth time increases from 2 to 48 h, the values o f Eg decrease from 3.21 to 3.11 eV. According to the bandgap energy (E_g) of the bulk ZnO, this results can be attributed to the optical confinement effect correspond to the size and length of NRs [10,38].

The photoluminescence (PL) spectra of different growth time of ZnO nanorods were also measured in order to investigate the influence of nanorods length. Fig. 8 shows the room-temperature PL spectra of various growth times (2, 6, 18, and 48 h) of ZnO nanorods. All nanorods show two distinctive emission bands. The first emission band is the UV arises from the band-edge of ZnO and the peak position at around 395 nm. It is attributed by the recombination of free excitons through an exciton-exciton collision [38]. The second emission was abroad and green emission centered at 580 nm, originated from the point defect such as oxygen vacancies [39,40]. It is remarkable in Fig. 8 that the intensity of the two bands of PL emission depends significantly on the length of the nanorods. An intriguing result here is that the relative intensity of the two PL bands depends on the length of the nanorods. The UV band peaked around 395 nm is strongly enhanced when the length of ZnO nanorods is reduction and the humps at around 580 nm decreases. Between the two extreme lengths, this intensity enhancement is roughly of a factor of 2.5.

Conclusion

ZnO nanorods have been prepared using a low-cost and convenient method by using wet chemical route, and were characterized by TEM, XRD, UV–vis absorption, and photoluminescence spectroscopy. TEM images confirmed the nanostructure for the prepared ZnO nanorods with different lengths and diameters which depend on the growth time. For growth time between 2 and 48 h, the diameter increased from 16 to 20 nm and the length from 50 to 150 nm. XRD patterns show that the ZnO NRs had remarkably

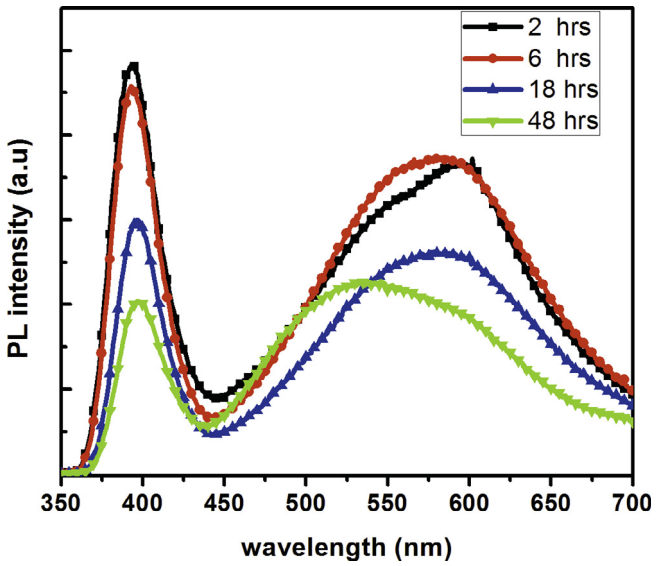

Fig. 8. Rom-temperature PL spectra of various growth times (2, 6, 18, and 48 h) of ZnO nanorods.

excellent crystal structure with a preferential orientation. Raman spectroscopy showed Raman silent modes at 273 and 538 cm^{-1}, which became activated with the presence of defects. Moreover, the PL spectrum showed that the relative intensity of ultraviolet (UV) and visible emission bands depend on the length of nanorods.

References

[1] Monge M, Kahn ML, Maisonnat A, Chaudret B. Room-temperature organometallic synthesis of soluble and crystalline ZnO nanoparticles of controlled size and shape. Angew Chem Int Ed Engl 2003;42:5321–4. https://doi.org/10.1002/anie.200351949.

[2] Prades JD, Cirera A, Ramon Morante J, Cornet A. Ab initio insights into the visible luminescent properties of ZnO. Thin Solid Films 2007;515:8670–3. https://doi.org/10.1016/j.tsf.2007.04.013.

[3] Meulenkamp EA. Synthesis and growth of ZnO nanoparticles. J Phys Chem B 1998;102:5566–72. https://doi.org/10.1021/jp980730h.

[4] Bendall JS, Visimberga G, Szachowicz M, Plank NOV, Romanov S, Sotomayor-Torres CM, et al. An investigation into the growth conditions and defect states of laminar ZnO nanostructures. J Mater Chem 2008;18:5259–66. https://doi.org/10.1039/B812867G.

[5] Borgohain K, Mahamuni S. Luminescence behaviour of chemically grown ZnO quantum dots. Semicond Sci Technol 1998;13:1154. https://doi.org/10.1088/0268-1242/13/10/017.

[6] Ravirajan P, Peiró AM, Nazeeruddin MK, Graetzel M, Bradley DDC, Durrant JR, Nelson J. Hybrid polymer/zinc oxide photovoltaic devices with vertically oriented ZnO nanorods and an amphiphilic molecular interface layer. J Phys Chem B 2006;110:7635–9. https://doi.org/10.1021/jp0571372.

[7] Sun XW, Huang JZ, Wang JX, Xu Z. A ZnO nanorod inorganic/organic heterostructure light-emitting diode emitting at 342 nm. Nano Lett 2008;8:1219–23. https://doi.org/10.1021/nl080340z.

[8] Wang G, Chen Y, Shen X, Li J, Wang R, Lu Y, et al. Reversibility and stability of ZnO-Sb_2Te_3 nanocomposite films for phase change memory applications. ACS Appl Mater Interfaces 2014;6:8488–96. https://doi.org/10.1021/am501345x.

[9] Debasis LQ. Bera, Photoluminescence of ZnO quantum dots produced by a sol–gel process. Opt Mater 2008;30:1233–9. https://doi.org/10.1016/j.optmat.2007.06.001.

[10] Musa I, Massuyeau F, Cario L, Duvail JL, Jobic S, Deniard P, Faulques E. Temperature and size dependence of time-resolved exciton recombination in ZnO quantum dots 243107-243107–3. Appl Phys Lett 2011;99. https://doi.org/10.1063/1.3669511.

[11] Ouldhamadouche N, Achour A, Musa I, Ait Aissa K, Massuyeau F, Jouan PY, et al. Structural and photoluminescence characterization of vertically aligned multiwalled carbon nanotubes coated with ZnO by magnetron sputtering. Thin Solid Films 2012;520:4816–9. https://doi.org/10.1016/j.tsf.2011.10.069.

[12] Musa I, Massuyeau F, Faulques E, Nguyen T-P. Investigations of optical properties of MEH-PPV/ZnO nanocomposites by photoluminescence spectroscopy. Synth Met 2012;162:1756–61. https://doi.org/10.1016/j.synthmet.2012.01.011.

[13] Rana AK, Aneesh J, Kumar Y, Arjunan MS, Adarsh KV, Sen S, Shirage PM. Enhancement of two photon absorption with Ni doping in the dilute magnetic semiconductor ZnO crystalline nanorods. Appl Phys Lett 2015;107:231907. https://doi.org/10.1063/1.4937583.

[14] Rana AK, Kumar Y, Rajput P, Jha SN, Bhattacharyya D, Shirage PM. Search for origin of room temperature ferromagnetism properties in Ni-Doped ZnO nanostructure. ACS Appl Mater Interfaces 2017;9:7691–700. https://doi.org/10.1021/acsami.6b12616.

[15] Sakurai M, Wang YG, Uemura T, Aono M. Electrical properties of individual ZnO nanowires. Nanotechnology 2009;20:155203. https://doi.org/10.1088/0957-4484/20/15/155203.

[16] Shirage PM. ZnO nano-flowers. Mater Today 2013;16:505–6. https://doi.org/10.1016/j.mattod.2013.11.007.

[17] Spanhel L, Anderson MA. Semiconductor clusters in the sol-gel process: quantized aggregation, gelation, and crystal growth in concentrated zinc oxide colloids. J Am Chem Soc 1991;113:2826–33. https://doi.org/10.1021/ja00008a004.

[18] Ozerov I, Nelson D, Bulgakov AV, Marine W, Sentis M. Synthesis and laser processing of ZnO nanocrystalline thin films. Appl Surf Sci 2003;212–213:349–52. https://doi.org/10.1016/S0169-4332(03)00100-4.

[19] Kong YC, Yu DP, Zhang B, Fang W, Feng SQ. Ultraviolet-emitting ZnO nanowires synthesized by a physical vapor deposition approach. Appl Phys Lett 2001;78:407–9. https://doi.org/10.1063/1.1342050.

[20] Podrezova LV, Cauda V, Stassi S, Cicero G, Abdullin KA, Alpysbaeva BE. Properties of ZnO nanorods grown by hydrothermal synthesis on conductive layers. Cryst Res Technol 2014;49:599–605. https://doi.org/10.1002/crat.201300372.

[21] Das R, Kumar A, Kumar Y, Sen S, Shirage PM. Effect of growth temperature on the optical properties of ZnO nanostructures grown by simple hydrothermal method. RSC Adv 2015;5:60365–72. https://doi.org/10.1039/C5RA07135F.

[22] Wu GS, Xie T, Yuan XY, Li Y, Yang L, Xiao YH, et al. Controlled synthesis of ZnO nanowires or nanotubes via sol–gel template process. Solid State Commun 2005;134:485–9. https://doi.org/10.1016/j.ssc.2005.02.015.

[23] Pacholski C, Kornowski A, Weller H. Self-assembly of ZnO: from nanodots to nanorods. Angew Chem Int Ed 2002;41:1188–91. https://doi.org/10.1002/1521-3773(20020402)41:7<1188::AID-ANIE1188>3.0.CO;2-5.

[24] Ahmed F. Growth and characterization of ZnO nanorods by microwave-assisted route: green chemistry approach. Adv Mater Lett 2011;2:183–7. https://doi.org/10.5185/amlett.2011.1213.

[25] Serrano J, Manjón FJ, Romero AH, Ivanov A, Cardona M, Lauck R, et al. Phonon dispersion relations of zinc oxide: Inelastic neutron scattering and *ab initio* calculations. Phys Rev B 2010;81. https://doi.org/10.1103/PhysRevB.81.174304.

[26] Manjón FJ, Marí B, Serrano J, Romero AH. Silent Raman modes in zinc oxide and related nitrides. J Appl Phys 2005;97:053516. https://doi.org/10.1063/1.1856222.

[27] Calzolari A, Nardelli MB. Dielectric properties and Raman spectra of ZnO from a first principles finite-differences/finite-fields approach. Sci Rep 2013;3. https://doi.org/10.1038/srep02999.

[28] Hoyer P, Eichberger R, Weller H. Spectroelectrochemical investigations of nanocrystalline ZnO films, Berichte Bunsenges. Für Phys Chem 1993;97:630–5. https://doi.org/10.1002/bbpc.19930970416.

[29] Nie JC, Yang JY, Piao Y, Li H, Sun Y, Xue QM, et al. Quantum confinement effect in ZnO thin films grown by pulsed laser deposition. Appl. Phys. Lett. 2008;93:173104. https://doi.org/10.1063/1.3010376.

[30] Bairamov BH, Heinrich A, Irmer G, Toporov VV, Ziegler E. Raman study of the phonon halfwidths and the phonon—plasmon coupling in ZnO. Phys. Status Solidi B 1983;119:227–34. https://doi.org/10.1002/pssb.2221190126.

[31] Arguello CA, Rousseau DL, Porto SPS. First-order raman effect in Wurtzite-type crystals. Phys. Rev. 1969;181:1351–63. https://doi.org/10.1103/PhysRev.181.1351.

[32] Tripathi N, Vijayarangamuthu K, Rath S. A Raman spectroscopic study of structural evolution of electrochemically deposited ZnO films with deposition time. Mater. Chem. Phys. 2011;126:568–72. https://doi.org/10.1016/j.matchemphys.2011.01.026.

[33] Calleja JM, Cardona M. Resonant Raman scattering in ZnO. Phys Rev B 1977;16:3753–61. https://doi.org/10.1103/PhysRevB.16.3753.

[34] Shen L, Bao N, Yanagisawa K, Domen K, Gupta A, Grimes CA. Direct synthesis of ZnO nanoparticles by a solution-free mechanochemical reaction. Nanotechnology 2006;17:5117–23. https://doi.org/10.1088/0957-4484/17/20/013.

[35] Zhang R, Yin P-G, Wang N, Guo L. Photoluminescence and Raman scattering of ZnO nanorods. Solid State Sci 2009;11:865–9. https://doi.org/10.1016/j.solidstatesciences.2008.10.016.

[36] Yang RD, Tripathy S, Li Y, Sue H-J. Photoluminescence and micro-Raman scattering in ZnO nanoparticles: the influence of acetate adsorption. Chem Phys Lett 2005;411:150–4. https://doi.org/10.1016/j.cplett.2005.05.125.

[37] Hassanien AS, Akl AA. Effect of Se addition on optical and electrical properties of chalcogenide CdSSe thin films. Superlattices Microstruct 2016;89:153–69. https://doi.org/10.1016/j.spmi.2015.10.044.

[38] Foo KL, Hashim U, Muhammad K, Voon CH. Sol–gel synthesized zinc oxide nanorods and their structural and optical investigation for optoelectronic application. Nanoscale Res Lett 2014;9:429. https://doi.org/10.1186/1556-276X-9-429.

[39] Lin B, Fu Z, Jia Y. Green luminescent center in undoped zinc oxide films deposited on silicon substrates. Appl Phys Lett 2001;79:943. https://doi.org/10.1063/1.1394173.

[40] McCluskey MD, Jokela SJ. Defects in ZnO. J Appl Phys 2009;106:071101. https://doi.org/10.1063/1.3216464.